

781

Z.P. BAŽANT

PORE PRESSURE, UPLIFT AND FAILURE
ANALYSIS OF CONCRETE DAMS

MS

CRITERIA AND ASSUMPTIONS FOR
NUMERICAL ANALYSIS OF DAMS

EDITORS: D.J. NAYLOR

K.G. STAGG

O.C. ZIENKIEWICZ

Proceedings of an International Symposium held at Swansea, U.K.

8 - 11 September, 1975

organised by

DEPARTMENT OF CIVIL ENGINEERING OF THE

UNIVERSITY COLLEGE, SWANSEA

in collaboration with the

BRITISH NATIONAL COMMITTEE ON LARGE DAMS

and the

LABORATORIO NACIONAL DE ENGENHARIA CIVIL, LISBON

under the patronage of

THE INTERNATIONAL COMMISSION ON LARGE DAMS

and its specialist Committee on the Analysis and Design of Dams

SUMMARY

The objective of the paper is a critical examination of the assumptions and equations which serve as basis for the calculation of pore pressures in concrete dams, as well as the concepts of effective stress and uplift pressure with regard to failure analysis. It is demonstrated that the water deficiency of concrete stemming from air-entrainment and self-desiccation due to hydration tremendously slows down the penetration of the front of hydraulic pressure. Spacing and width of continuous cracks have a major effect on the penetration rate. Drying affects only a shallow layer at downstream face. It is shown that, due to anisotropy of the micro-stress state in hindered adsorbed water layers, the effective uplift area should be distinctly less than 1.0 (about 0.9), even if over 99% of the weakest cross section passes through water. Tests of deformation due to pore pressure are shown to be incapable of providing the value of the uplift area and a value of 1.0 is shown to be most reasonable for strain calculations, unless a two-phase medium model is developed. The progressive nature of fracture must be taken into account in calculations of dam failure as well as test data evaluation. Concrete in dams cannot fail by shear (sliding) without volume expansion (microcracking), and so temporary suction is produced in the vicinity of failure surface. In the approximate nonlinear triaxial stress-strain relations for concrete, the effective stress based on effective porosity $n' = 1.0$ may be used for the elastic stress increments, while in the expressions for inelastic strains the (non-incremental) effective stress based on the actual n' should be used. A rigorous formulation in terms of an inelastic two-phase medium is also indicated.

INTRODUCTION

Gradients of pore pressures produce significant distributed loads (body forces) within concrete dams. These loads, which are usually called uplift forces, must be resisted by the solid microstructure of concrete and can lead to a sliding failure or an overturning failure of the dam. Prediction of pore pressures and uplift forces is, therefore, of considerable

importance in the design of gravity dams. Catastrophies which were clearly attributed to uplift forces occurred already in the 19th century and keen attention has ever since been devoted to the question of uplift. However, despite research efforts spanning over 70 years, certain questions still remain unanswered. They include: Should uplift be allowed for in joints and cracks only or within intact concrete? How should the pore pressures be calculated? Over what fraction of the total area of a given cross section are the pore pressures applied? How should the deformations and failure due to pore pressure be determined? The following analysis will address these and other related questions, and attempts to clarify several controversial points will be made.

DETERMINATION OF PORE PRESSURES

In greatest generality, diffusion of any substance in an isotropic porous solid at negligible temperature gradients is described, according to irreversible thermodynamics, by the relation:

$$\underline{J} = -c^* \text{grad } \mu \quad (1)$$

in which \underline{J} = mass flux vector (whose components represent masses that pass through the sides of a unit cube in a unit time), μ = Gibb's free energy per unit mass (also called chemical potential), c^* = coefficient that may, in general, depend on state variables. Eq. 1 may be adopted as the common ground for the diffusion laws of water in both the saturated and non-saturated concrete. The effects of temperature will be neglected in this study.

Saturated Concrete.

It may be assumed that solute concentrations gradients have a negligible effect on water diffusion. Then, for saturated concrete at uniform temperature, $\mu = p/\rho_w + \mu_0$ [5] where p = pore pressure in excess of atmospheric pressure [3], ρ_w = specific mass of liquid water ($\sim 1000 \text{ kg/m}^3$), μ_0 = constant (depending on temperature). Eq. 1 may then be reduced to the familiar Darcy's law:

$$\underline{J} = -\rho_w c \text{grad}(p/g_w) \quad (2)$$

in which $c = c^* g_w / \rho_w^2$; g_w = unit weight of liquid water ($\sim 9806 \text{ N/m}^3$); p/g_w = hydraulic head (dimension of length); c = permeability (dimension of m/sec). The capillary water content, w , defined as the mass of capillary water per m^3 of concrete, is related to pore pressure p :

$$dw/\rho_w = \beta dp \quad (3a)$$

in which β = compressibility of capillary water in concrete, with account of porosity.

The change in water content is related to the flux field by the equation of conservation of mass: $\text{div } \underline{J} = -\partial w / \partial t$. However, if the hydration reaction proceeds simultaneously with diffusion, this equation must be corrected for the amount of water, w_h , that is withdrawn from the pores of cement paste due to the hydration reaction; i.e.

$$\text{div } \underline{J} = -\frac{\partial w}{\partial t} + \frac{\partial w_h}{\partial t} \quad (3b)$$

In some recent works it has been assumed [1] that w_h equals the amount of chemically combined water. However, this is incorrect because the volume of cement gel is larger than the volume

* Professor of Civil Engineering, Northwestern University, Evanston, Illinois, 60201, USA.

of anhydrous cement (about twice as large). On the other hand, w_h is not zero because the volume of cement gel is less than the combined volume of water and anhydrous cement from which the cement gel was combined. Consequently, the volume of capillary pores decreases with hydration and the part of the chemically combined water which initially occupied the lost pore space Fig.1 must be excluded from the water withdrawn from the pore space by hydration. Powers [25] has estimated that the amount of water, w_h , that has been withdrawn from the pores of cement paste is about 28% of the amount of chemically combined water, and since the latter equals about 22% of the weight of cement (after prolonged hydration), the water deficiency represents about $28\% \times 22\% = 6.2\%$ of the weight of cement. For lean dam concrete (without pozzolans) containing 112 kg of cement per m^3 of concrete, there is thus, after prolonged hydration, a water deficiency of $w_h = 0.062 \times 112 \approx 7$ kg of water per m^3 of concrete, approximately. (For recent concretes with pozzolans [20], containing as little as 43 kg of cement per m^3 , the water deficiency is about 3 kg/ m^3 .) The foregoing value may be used as the final value, $w_h = w_h^\infty$. The time variation may be taken in the form $w_h = w_h^\infty f(t)$ where $f(t)$ is an increasing function with $f(0) = 0$ and $f(\infty) = 1$, possibly of the same form as the function defining strength increase with age. To account for the changes in hydration rate due to temperature changes, t in $f(t)$ may be replaced by the equivalent hydration period, t_e [3-5].

Substituting \underline{J} and dw from Eqs. 2 and 3a into Eq. 3b, one gets $\beta \rho_w \frac{\partial p}{\partial t} = \text{div}[c \rho_w \text{grad}(p/\beta g_w)] + \frac{\partial w_h}{\partial t}$, and noting further that c , as well as ρ_w and β , is almost constant within the range of p -values of interest, it follows:

$$\frac{\partial p}{\partial t} = C \nabla^2 p - \frac{1}{\beta \rho_w} \frac{\partial w_h}{\partial t} \quad \text{with} \quad C = \frac{c}{\beta g_w} \quad (4)$$

in which $\nabla^2 = \text{div grad} = \text{Laplace operator}$, and $C = \text{diffusivity of pore water in saturated concrete (dimension } m^2/\text{sec)}$; $w_h = \text{function of time that must be prescribed}$. Eq. 4 is the familiar linear diffusion equation and methods of its solution are well known. However, the numerical values of material parameters deserve some discussion.

Permeability is easier to measure than is diffusivity. For lean concretes which are typical for dams, permeability c is of the order of 10^{-10} m/sec and a typical value is

$$c \approx 50 \times 10^{-12} \text{ m/sec.} \quad (5)$$

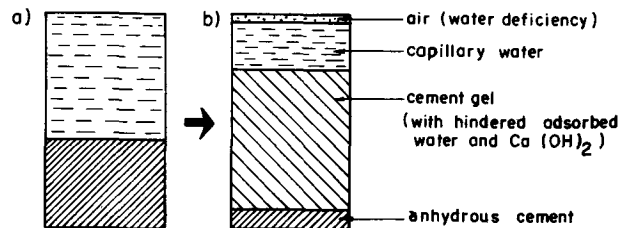


Fig. 1 Change of Capillary Pore Space and Water Deficiency Caused by Hydration

For a concrete with 112 kg of cement per m^3 of concrete, Carlson has observed the values 175, 60 and 40×10^{-12} m/sec at ages 3, 12, and 24 months, respectively [12]. For the newly introduced very lean concretes, with as little as 43 kg of cement per m^3 , 70 to 200 kg/ m^3 pozzolans and 80 to 150 kg/ m^3 water, the permeabilities at age of 3 months range between 6×10^{-12} m/sec [20]. These permeabilities are several orders of magnitudes higher than those for dense structural concretes; but permeability of intact concrete has little effect on leakage through gravity dams, as compared with the effect of cracks and joints.

To determine diffusivity on the basis of permeability, compressibility β must be estimated. If the solid structure of concrete were perfectly rigid, β would equal $n\beta_w$; $n\beta_w = \text{bulk compressibility of liquid water (about } 0.00049 \text{ m}^2/\text{MN at room conditions)}$ and $n = \text{capillary porosity} = \text{volume of freely compressible water} = \text{volume of capillary pores per unit volume of concrete}$. Not all water in concrete, not even all evaporable water, should be included under n . The non-evaporable, chemically bound water must be excluded because its molecules are part of the solid structure. The water molecules in hindered adsorbed layers [5], even though they are evaporable, should probably be also excluded, at least in part, because their equilibrium spacing is fixed by the molecular structure of the solid surfaces. This leaves the capillary water and unhindered adsorbed water, which is all water that is contained in pores more than 10 molecules (26 Å) in thickness. The weight of the freely compressible water equals the total weight of water in the mix, minus about 30% to 40% of the weight of cement before hydration (in a mature concrete). Clearly, n is decreasing with age (degree of hydration), and so does β . (Hence, diffusivity must be increasing with age faster than permeability, but no data seem to be available to this effect.)

In determining β one must further include the dilation of pore space due to dilation of solid structure produced by pore pressure. This quantity depends on whether this dilation occurs at constant total stress in the porous material, or at constant effective stress, or at some other condition. Since the overburden of a given element of concrete remains constant, a constant total stress is probably the most representative condition. It has been derived for saturated sand that $\beta = n\beta_w + (1-2n)C_b$ where $C_b = \text{bulk compressibility of the porous material at constant pore pressure}$ ($C_b = 1/K$, $K = \text{bulk modulus}$); see Eq. 53 of Ref. [8]. For concrete, this relation certainly does not hold exactly, but probably it can be applied as an approximation. Considering concrete of strength 24 MN/ m^2 (3500 psi), elastic modulus $E = 23000 \text{ MN}/m^2$ (3 336 000 psi) and Poisson ratio $\nu = 0.18$, one gets $C_b = (1-2\nu)/E = 27.8 \times 10^{-6} \text{ m}^2/\text{MN}$. Furthermore, considering concrete of 112 kg of cement and 80 kg of water per m^3 , and an aggregate of porosity of 1%, it may be estimated that $n \approx 0.05$. The foregoing approximate formula for β then yields $\beta \approx (0.05 \times 490 + 0.9 \times 27.8) 10^{-6} \approx 50 \times 10^{-6} \text{ m}^2/\text{MN}$. Note that this value is close to C_b , bulk compressibility of concrete.

The preceding derivation confirms the empirical observation of Murata [21] that compressibility β in the relation of diffusivity to permeability should be taken approximately as the bulk compressibility of concrete. A typical value of permeability of a 1-year old lean dam concrete is 50×10^{-12} m/sec, and this yields, according to Eq. 4,

$$C \approx 10^{-6} \text{ m}^2/\text{sec} \quad (6)$$

which is the upper limit of the diffusivities of concretes as determined by Murata [21] from penetration depth tests.

The depth of penetration of hydraulic pressure for $\dot{w}_h = 0$, pertaining to one-dimensional diffusion into an infinite space $x \geq 0$ exposed to water of pressure p_0 at $x = 0$ for $t \geq 0$, may be found from the following well-known solution of Eq. 4 [13]:

$$p(x,t) = p_0 \operatorname{erfc}(\xi) = p_0 \frac{2}{\sqrt{\pi}} \int_{\xi}^{\infty} e^{-s^2} ds, \quad \xi = \frac{x}{2\sqrt{Ct}} \quad (7)$$

in which erfc = complementary error function. Defining the depth of penetration as the distance from the surface to the point where $p = p_0/100$, one can find from a table of the error function that $\xi = 1.820$. For example, consider a 100m-high gravity dam which is 80 m thick at the base and neglect the water deficiency due to hydration, setting $\dot{w}_h = 0$. Then, the time (after filling of the reservoir) needed for the penetration of the full thickness of dam is

$$t = \frac{x^2}{4C\xi^2} = \frac{80^2}{4 \times 10^{-4} \times 1.82^2} \text{ sec} \approx 56 \text{ days} \quad (\text{for } C = 10^{-4} \text{ m}^2/\text{sec}) \quad (8)$$

This is a relatively short time, which contradicts the fact that only relatively small pressures have been observed within the mass of concrete in dams [26, 15, 17, 10] (while within cracks and cracked construction joints high pressures are observed [22]). In reality, there indeed exist phenomena which tremendously prolong the penetration time.

The water deficiency w_h created by hydration is one such phenomenon. An approximate solution of Eq. 4, valid for sufficiently long time periods, may be obtained by assuming that hydration becomes nearly complete before the hydraulic pressure front arrives. Thus, air-filled voids are produced by hydration in concrete before the arrival of the front. This phenomenon is called self-desiccation and is manifested by a several percent drop of humidity below 100 percent [23]. It is thus clear that the build-up of hydraulic pressure in concrete requires not only the supply of water necessary for elastic compression or pore water, but also the supply of water necessary for filling the pores. The latter amount is much higher than the former one and must have an overriding effect on the rate of penetration of the hydraulic pressure front. Assuming that the rate of advance of the front is diminished by orders of magnitude, the pressure distribution between the surface and the front will nearly equal the stationary distribution for the case of immobile front, which is a linear distribution. Therefore, the amount of water (per m^3) that must be supplied to the front in time interval dt is $Jdt = \rho_w c (p_0/g_w x) dt$. Furthermore, because water diffusion in non-saturated concrete is very slow, the water deficiency just ahead of the front should be almost the same as that far ahead of the front. Consequently, $Jdt = w_h dx$, where dx = advance of the front during dt , w_h = water deficiency per m^3 , estimated in the foregoing. Hence, $x dx = (p_0 c \rho_w / w_h g_w) dt$. Integration gives $\frac{1}{2} x^2 = p_0 c \rho_w / w_h g_w t$, and so the time of penetration to depth $x = 80$ m at the base of a 100m-high dam is

$$t \approx \frac{w_h g_w x^2}{\rho_w 2 p_0 c} = \frac{7}{1000} \frac{80^2}{2 \times 100 \times 50 \times 10^{-12}} \text{ sec} \approx 142 \text{ years} \quad (9)$$

considering the permeability to be 50×10^{-12} m/sec. Eq. 9 is not valid in a region close to the upstream face because hydration is not complete before the arrival of pressure front. In this region it is possible that pressure first builds up and is subsequently reduced to zero (unsaturated condition) due to the term \dot{w}_h in Eq. 4, as is indeed observed experimentally [5].

Another reason for the initial lack of saturation of concrete is air-entrainment, necessary for good workability at low water and cement contents. Typically, air-entrainment represents 6% of the volume of concrete, which indicates water deficiency of 60 kg/m^3 , in addition to 7 kg/m^3 due to hydration. According to Eq. 9, the penetration time is then extended to $t = 1360$ years, a value which is practically irrelevant, of course. The effect of air-entrainment on the penetration time has been previously analyzed by Carlson [12] and he obtained a similar result. The depth of penetration which is reached within a 100-year period (3156×10^6 sec) is, according to Eq. 9,

$$x = \left(\frac{\rho_w}{w_h} \frac{2 p_0 c}{g_w} t \right)^{\frac{1}{2}} = \left(\frac{1000}{60 + 7} 2 \times 100 \times 50 \times 10^{-12} \times 3156 \times 10^6 \right)^{\frac{1}{2}} \text{ m} = 21.7 \text{ m} \quad (10)$$

which means that only about $\frac{1}{4}$ of the dam thickness could receive hydraulic overpressure if concrete remained free of seepage channels such as cracks and leaking construction joints (Fig. 2). This seems to agree with measurements of pore pressures in dams [26, 15, 17, 10].

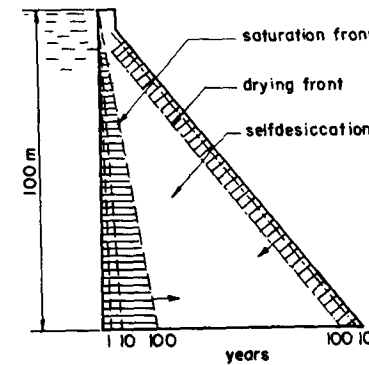


Fig. 2 Advance of the Fronts of Saturation and of Drying in an Ideal Dam Having No Cracks, No Cracked Joints, and No Drainage (for a Typical Concrete)

Eqs. 9 and 10 are based on the assumptions that concrete is intact (uncracked), no seepage channels through the dam exist, and no upward diffusion from the bedrock takes place. However, even if these assumptions are inapplicable, the value of diffusivity is clearly irrelevant for the build-up of pore pressures inside the dam, except very near the upstream face (or near the seepage channels).

Regarding the effect of deformations of concrete on diffusion, Eqs. 3a and 4 include only the deformation due to pore pressure, but not the deformation due to loads applied on concrete. This effect, which must be as significant as the deformation due to pore pressure, can be rigorously formulated only with the help of a two-phase medium model (see Eqs. 40 in the

sequel, which would replace Eq. 3 and yield a diffusion equation more involved than Eq. 4). However, in practice the changes of pore pressure due to deformation do not appear to be too important because they are small in comparison with the effect of initial water deficiency of concrete upon the subsequent build-up of pore pressures.

Non-Saturated Concrete.

As has been mentioned, concrete of the dam tends to remain unsaturated for a long time because of self-desiccation and air-entrainment. Further loss of water occurs by drying from the downstream face exposed to the atmosphere. A detailed study of water diffusion in non-saturated concrete has been given in Ref. [3] and only the most pertinent facts will be reviewed herein.

The problem can be formulated either in terms of the specific water content, w , or in terms of capillary tension or surface tension, or in terms of relative vapor pressure h in the pores (pore humidity). The latter variable is probably most convenient because, among other reasons [3], h is at the same time a characteristic of the environment. Assuming ideal gas approximation for water vapor, the Gibbs free energy per unit mass of pore water may be shown to equal $\mu = (R/M) T \ln h + \mu_0$ where R = gas constant, M = molecular weight of water, T = absolute temperature. Substituting μ in Eq. 1, it follows:

$$\underline{J} = -c' \text{ grad } h \quad (11)$$

in which $c' = (R/M)T c^*/h$ [3]. The change of h is related to total water content \bar{w} per m^3 as $dh = kd\bar{w} + dh_g$ or $d\bar{w} = (dh - dh_g)/k$ where dh_g = increment of self-desiccation during time dt and $k = \partial\bar{w}/\partial h$ = inverse slope of the desorption (or sorption) isotherm of concrete. Substituting this expression for $d\bar{w}$, together with Eq. 11, into the mass continuity relation $\partial\bar{w}/\partial t = -\text{div } \underline{J}$, and assuming k to be constant, one gets:

$$\frac{\partial h}{\partial t} = \text{div } (C' \text{ grad } h) + \frac{\partial h_g}{\partial t} \quad (\text{at } T = \text{const.}) \quad (12)$$

in which $C' = kc' = k(c^*/h) RT/M$ = diffusivity of water in non-saturated concrete. Self-desiccation h_g , as well as C' , is a given function of the equivalent hydration period t_e defined by $dt_e = \beta_h dt$ where β_h is a given function of h ; h_g decreases from 100% to about 95% to 98% as hydration progresses, and C' continually decreases with hydration [3]. The most important property of C' (see Ref. 3) is its marked dependence on h , which makes the diffusion problem strongly nonlinear; C' drops about 20-times when passing from 90% to 60% pore humidity and remains then constant down to about 20%. This is expressed by the formula [2, 3]:

$$C'(h) = C'_1 \left(\alpha_0 + \frac{1 - \alpha_0}{1 + \left(\frac{1-h}{1-h_c}\right)^n} \right) \quad (13)$$

where $\alpha_0 \approx 0.05$, $h_c = 0.75$, $n=6$. Diagrams for prediction of drying of simple bodies based on Eqs. 12 and 13 are available in Ref. [3]. According to Ref. [3], a typical value of C'_1 for a dense concrete (of low water-cement ratio) is $0.25 \times 10^{-9} m^2/\text{sec}$; but for lean dam concretes with high water-cement ratio a more typical value probably is (according to Aleksandrovskii's

[1] data):

$$C'_1 \approx 10^{-9} m^2/\text{sec}. \quad (14)$$

Compared to the diffusivity in saturated concrete (Eq. 6), this is a far smaller value (400 000-times smaller). The reason for this difference is the fact that much water needs to flow into unsaturated pores to change pore humidity appreciably but extremely little water needs to be forced into saturated pores to change hydraulic pressure significantly. Consequently, the spreading of a drying front into a concrete dam is extremely slow. For example, according to Eq. 8, if environmental humidity is 90% it would take 61 000 years for a drying front to spread all the way across the 80-m base of dam, and if the environmental humidity is below 60%, it would take up to 20-times longer. These times are, of course, practically irrelevant. The depth of penetration of the drying front which can be reached in a 100-year period (3156×10^6 sec) is, according to Eq. 7 (and neglecting self-desiccation):

$$x = 2\sqrt{C'_1 t} = 2 \times 1.82 \sqrt{10^{-9} \times 3156 \times 10^6} = 6.47 \text{ m} \quad (15)$$

if the humidity is 90%, and roughly $\sqrt{20}$ -times less, or 1.45 m, if it is below 60%. Such depth of penetration is insignificant for gravity dams, although it is significant for arch dams of smaller height.

Permeability of non-saturated concrete, defined by Eq. 11, may be determined from diffusivity C' using the relation given below Eq. 12, which yields

$$c' = C'/k \quad (16)$$

To this end, it is necessary to determine k . Empirically, the slope of desorption isotherms, $1/k$, at advanced hydration and at high h -values is about $(2/3)w_{ev}$ (per 100% humidity) w_{ev} = total water content (per m^3), plus water deficiency due to air-entrainment, and less the chemically bound water, the latter of which represents about 22% of the weight of cement at advanced stages of hydration. For the previously considered concrete with 112 kg of cement per m^3 , water content 125 kg/m^3 and 6% air-entrainment, $w_{ev} = 0.667 \times 125 + 0.06 \times 1000 - 0.22 \times 112 = 120 \text{ kg}/m^3$. Hence, $1/k \approx 120 \text{ kg}/m^3$ (per 100% humidity drop), and so Eq. 16 provides, for the high humidity range,

$$c' \approx 120 \times 10^{-9} \frac{\text{kg}}{\text{m}^3 \text{ sec}} \quad (\text{at } h \rightarrow 1) \quad (17)$$

Direct measurements of permeability of non-saturated concrete are scant. For cement mortars of water-cement-sand ratio 0.8:1:5.2 Wierig [30] observed, at humidities below 50%, values of the order of $1.4 \times 10^{-9} \text{ kg}/\text{m}^2 \text{ sec}$ at 1 year of age and about 6-times more at 3 days of age. For concretes of cube strength around 42 N/mm^2 (6100 psi) with 340 kg/m^3 of concrete and water-cement-aggregate ratio 0.6:1:5.32 he got 6×10^{-9} at 7 days of age. Considering that Eq. 17 applies for very lean concretes of high water-cement ratios, and that for high humidity c' may be about 20-times larger, Wierig's data seem to agree with Eq. 17.

Saturation Boundary.

At the saturation boundary (interface between saturated and non-saturated concrete), the normal component J_n of the water flux \underline{J} must be the same on each side of the interface. Recalling Eqs. 2 and 11, $J_n = -\rho_w c' \text{ grad}_n (p/g_w) = -c' \text{ grad}_n h$, i.e.

$$\text{grad}_n \left(\frac{p}{\rho_w} \right) = \alpha_n \text{grad } h, \quad \text{with } \alpha_n = \frac{c'}{c \rho_w} \quad (18)$$

Considering the values given in Eqs. 5 and 17, the gradient ratio is obtained as

$$\alpha_n \approx 2.4 \text{ m} \quad (19)$$

It is interesting to determine the permeability c^* in the fundamental Eq. 1 from the permeabilities that yielded this value of α_n (Eqs. 5 and 17). The relations $c^* = c \rho_w^2 / \rho_w$ and $c^* = c' h M / RT$ (with $h \rightarrow 1$) furnish $c^* = 5100 \times 10^{-12} \text{ kg sec/m}^3$ for saturated concrete and $c^* = 0.87 \times 10^{-12} \text{ kg sec/m}^3$ for non-saturated concrete at $h \rightarrow 1$. Thus, it is apparent that for the concretes considered, permeability c^* (Eq. 1) increases about 6000-times on reaching saturation. Physically, this may be explained by the fact that very lean dam concrete contains relatively large capillary pores, which become filled quite abruptly when h reaches 100%. Such abrupt filling must largely increase the permeability because water diffusion in non-saturated concrete must occur mostly by diffusion in adsorbed water layers and continuous capillaries, rather than by diffusion of water vapor.

On the other hand, the permeability for mature dense cement pastes in saturated state is much less than that in Eq. 5 (10^{-15} to 10^{-12} m/sec [24], for water-cement ratios 0.3 to 0.7) and may even be nearly continuous when passing from a non-saturated state to a saturated state (cf. p. 13 of Ref. 3). In that case it can be shown [3] that $\alpha_n = (RT/M) \rho_w / \rho_w \approx 14 \text{ 050 m}$, which tremendously exceeds the value in Eq. 19. The physical reason for this large value is that the tension in adsorbed water layers and capillary water is very large (e.g., equivalent to the hydraulic head of 6050 m if $h = 65\%$ and 25°C).

The value of gradient ratio α_n governs the location of saturation boundary within the thickness of dam when the final, stationary state of water diffusion is reached. (In a flawless dam, this state can never be reached within the service lifetime except if the dam is relatively thin, as in the case of arch dams of low height.) Denoting by x_g the distance of the saturation boundary from the upstream face, by L the thickness of dam, by p_0 the pressure at upstream face, by h_0 the environmental humidity, and assuming that c' is constant within the range of h -values in the pores, it follows from Eq. 18 that $(p_0 / \rho_w x_g) = \alpha_n (1 - h_0) / (L - x_g)$, i.e. $x_g = L / [1 + \alpha_n (1 - h_0) \rho_w / p_0]$. For lean dam concretes considered (Eq. 18), and for a hydraulic head of 100 m and $h_0 = 65\%$, one obtains $x_g = 0.99 L$, while for very dense concretes with $\alpha_n = 14 \text{ 050 m}$, one obtains $x_g = 0.020 L$ [3]. It is probably the former value which is much closer to reality for dam concretes; but the discrepancy between the last two values of x_g indicates that the location of the saturation boundary in the final, stationary state is extremely sensitive to the ratio of permeabilities in the saturated and non-saturated states and can vary widely from concrete to concrete, the same as the permeabilities do.

An important experiment with regard to the location of saturation boundary has been carried out long ago by Carlson and Davis [11]. A pipe of 152 mm diameter and 2.44 m long was filled by concrete and one end was immersed in water of hydraulic head 70.3 m while the other end was exposed to air of relative humidity $h_0 = 50\%$. The pore pressure was measured by Bourdon gages, the first one being located 102 mm from the immersed end. At early ages small pore pressures were registered by the first gage, but within seven years all gages including to the first one registered zero. One possible explanation (suggested already by

Powers [25] and analyzed also in [3]) is that at 7 years the diffusion process approached a steady state for which the saturation boundary is located closer than 102 mm (or 0.0625 of the pipe length) to the immersed end. According to the previously calculated values of x_g , this may have been indeed possible if the concrete was rather dense and impermeable (and, of course, free of cracks, which was probably assured by confinement in the pipe). Self-desiccation has undoubtedly also contributed to reducing the pore pressures.

For numerical analysis, finite elements based on both saturated (Eq. 4) as well as non-saturated (Eq. 12) condition must be formulated. Each time step is iterated; a switch between saturated and non-saturated case must be made as soon as p drops below zero or h exceeds 1.0.

THE QUESTION OF UPLIFT WITHIN CONCRETE

In the analysis of gravity dams, it is of considerable interest to know how much the tensile stresses in the solid microstructure are increased by the presence of pressure within the pores. Because the total vertical normal stress in concrete is independent of pore pressure, an increase of pore pressure must result in a decrease of tension in the solid microstructure, so as to preserve equilibrium. In horizontal cross sections, the pore pressure acts upwards upon the overlying concrete and is therefore called uplift pressure. The magnitude of the resultant of this pressure plays an important role in the analysis of the safety of the dam against overturning and sliding, as well as in the prediction of the safety against cracking and local failure of concrete.

Two different cases may be distinguished: uplift pressures within cracks (or cracked construction joints) and uplift pressures in cross sections passing through intact concrete. The former case requires no theoretical questions to be settled, although the location, extent, and opening of cracks may be difficult to predict in practice; but the theoretical picture of the second case is still partly clouded, despite many years of research. Only the latter case will be considered herein.

Equilibrium in a Two-Phase Medium.

Having introduced pore pressure as an independent variable, concrete should be properly treated as a porous two-phase medium, the basic theory of which has been developed by Biot (see, e.g., [9]). The basic kinematic variables of the two-phase medium are cartesian displacement components u_i of the solid phase and u_i^F of the fluid phase ($i = 1, 2, 3$). Since shear stresses in the fluid phase are negligible, the deviatoric deformations of the solid phase are not affected by the presence of the solid phase, and so the pore pressure p appears only in the volumetric stress-strain relations. The volumetric strains of the solid and fluid phases are defined as $\epsilon = \text{div } u_i$ and $\epsilon^F = \text{div } u_i^F$.

The following question now appears. What are the stresses σ^S in solid and σ^F which are associated with ϵ and ϵ^F so that $\sigma^S d\epsilon + \sigma^F d\epsilon^F$ would be the correct work expression? The work of fluid flow per unit material element at $\delta\epsilon = 0$ equals $-p \delta V_F$ where $\delta V_F = n \delta \epsilon^F$ = volume of water that flows out of the unit element. Thus, $\sigma^F \delta \epsilon^F = -p(n \delta \epsilon^F)$, which provides

$$\sigma^F = -np \quad (20)$$

as the only admissible definition of σ^F . Eq. 20 represents the resultant of pressure p over a unit cross section of porosity n , which happens to be the statically average porosity of a cross section that is perfectly planar (rather than microscopically sinuous) (section AA' in Fig. 4). The stress in the solid phase, σ^S , must then represent the resultant of the

stresses acting over the remaining area, $1-n$, of the perfectly planar unit cross section. It is thus clear that the stress associated with e is neither the effective stress σ' , nor the total stress σ .

The differential equations of equilibrium of a porous two-phase medium read [9]:

$$\sigma_{ij,j}^S + \rho^S g_i + b(\dot{u}_i^F - \dot{u}_i) = 0 \quad (21)$$

$$\sigma_{,i}^F + \rho^F g_i - b(\dot{u}_i^F - \dot{u}_i) = 0$$

in which the subscripts refer to cartesian coordinates x_i ($i = 1, 2, 3$), a subscript following a comma denotes a derivative, and the summation rule is implied; σ_{ij}^S = stress tensor in the solid phase ($\sigma_{kk}^S/3 = \sigma$); ρ^S and ρ^F = average mass densities of the solid and fluid phases; g_i = acceleration vector (gravity acceleration); b = viscosity parameter; $b(\dot{u}_i^F - \dot{u}_i)$ = flow drag of the fluid phase upon the solid phase; and the superimposed dot designates a time derivative. Summing Eqs. 21, one obtains

$$\sigma_{ij,j} + \rho g_i = 0 \quad (21a)$$

or alternatively

$$\sigma_{ij,j}^S + \rho g_i + U_i = 0 \quad (22)$$

in which $\rho = \rho^S + \rho^F$ = total mass density of the material, $\sigma_{ij} = \sigma_{ij}^S + \delta_{ij}\sigma^F = \sigma_{ij}^S - \delta_{ij}np$ = tensor of total stress (δ_{ij} = Kronecker delta), ρg_i = total weight of material per unit volume; and

$$U_i = \sigma_{,i}^F = -(np)_{,i} = -\text{grad}_i(np) \quad (23)$$

The well-known effective (volumetric) stress, σ' , represents the resultant of microstresses in the solid phase taken over a unit cross section which is macroscopically planar but microscopically sinuous, so that the weakest cross section (i.e., the section having the minimum possible area of solids within the cross section) be obtained. If the area of pores in this cross section is denoted as n' (see BB' in Fig. 4), one has

$$\sigma' = \sigma + n'p, \quad \sigma'_{ij} = \sigma_{ij} + \delta_{ij} n'p \quad (24)$$

in which σ'_{ij} = effective stress tensor and n' = effective porosity (or boundary porosity [29 superficial porosity [18]]). (In granular materials, σ'_{ij} characterizes the intergranular contact forces.) Note that σ'_{ij} is positive for tension while p is positive for compression. Substitution for σ_{ij} from Eq. 24 into Eq. 21a yields

$$\sigma'_{ij,j} + \rho g_i + U_i = 0 \quad (25)$$

with

$$U_i = -(n'p)_{,i} = -\text{grad}_i(n'p) \quad (26)$$

Eqs. 22 and 25 represent the differential equations of equilibrium written in terms of the stresses in the solid phase and the effective stresses, respectively. In both of these equations, the total mass density is used and U_i or U_i' represent an additional body force (per unit volume), which may be called the average or effective uplift force, respectively. Eqs. 23 and 26 indicate the connection between the uplift force and the pore pressure, while the quantity $n'p$ in Eq. 26 expresses what is known as uplift pressure. By analogy to this term, n' is called uplift area.

Note that, in general, the uplift force U_i is not vertical because $\text{grad } p$ is not vertical (Eq. 26). In fact, for the typical pore pressure distributions in dams, uplift forces within the dam have sizable horizontal components (as was pointed out long ago by Fillunger; cf. Ref. 3). Denoting by H_u the resultant of all these horizontal components within the dam (Fig. 3), it may be easily shown that the horizontal hydrostatic resultant H which the reservoir exerts upon the upstream face of dam is diminished precisely by H_u , due to pore pressures which act at the face against the reservoir. Thus the horizontal component of uplift accounts for the fact that the point of application of a part of the total horizontal hydrostatic force H is gradually being transferred into the dam as the pore pressures are building up in the dam. (The effect of H_u has been a subject of prolonged polemics between 1910 and 1935.)

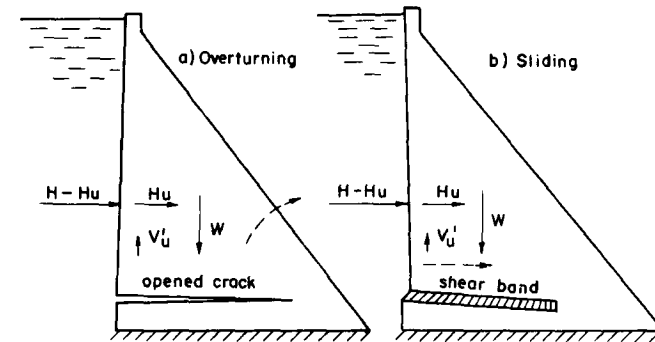


Fig. 3 Basic Modes of Dam Failure (W = weight of all concrete with pore water, V_u' = resultant of effective vertical uplift forces U').

The main purpose of using the concepts of effective stress and uplift pressure is to be seen in the convenience of formulating the failure criterion. Particularly simple is the case of saturated sand, a material for which the effective stress was defined first; here $n' = 1$ and the condition of no failure is $\sigma' \leq 0$ (with $\sigma' = \sigma + p$). In the case of a porous solid consisting of bonded grains (e.g., certain porous sedimentary rocks, Fig. 4), $n' < 1$ and

$$\sigma - f_b' \leq 0 \quad \text{or} \quad \sigma + n'p - f_b' \leq 0 \quad (27)$$

where f'_b = strength parameter characterizing the strength of intergranular bonds. However, this condition, in contrast with that for sand ($n' = 1$), is no longer exact, because f'_b in general depends, in an unknown manner, on p . For example, p affects the lateral stress in the material of intergranular joints (Fig. 4) and this in turn must affect their strength, f'_b , although possibly to a small degree. Most generally, for any porous material, the (volumetric) condition of no failure may be written as

$$F_1(\sigma_{ij}, p) = F_2(\sigma'_{ij}, p) = \sigma + n'(p)p - f'_b(\sigma'_{ij}, p) \leq 0 \quad (28)$$

where n' is also a function of p . When this is the case, it is of no help to introduce the effective stress. Either function F_1 or function F_2 must be determined experimentally and neither way is simpler than the other.

Non-saturated Concrete.

In non-saturated concrete the fluid consists of air with water vapor, capillary water, and adsorbed water. (Properly, the material should be treated as a multiphase system.) The pore pressure is negative, i.e. a tension, whose magnitude is very large (of the order of hundreds of atmospheres) and results in a compression of the solid microstructure, which is known as shrinkage (instantaneous shrinkage [5]). Since the effect of pore pressure is accounted for in terms of shrinkage, it would be an incorrect duplication if body forces U'_i and pore pressures p' (negative "uplift") were considered together with the corresponding effective stress σ' . In fact, according to the theorem of equivalence of inelastic strains and body forces (body force analogy, see Sec. 5.4 of Ref. 5), the effect of a change in body forces U'_i is equivalent to the effect of the shrinkage increments.

In non-saturated concrete, the situation is of the type described by Eq. 28. The effective area for the (negative) pressure in capillary water and adsorbed water is strongly dependent on the pressure itself, the resultant is further affected by (positive) disjoining pressures in hindered adsorbed layers, and the strength of interparticle bonds depends on the degree of water saturation in the long narrow gaps between the gel particles (Fig. 6). Thus, it is clear that the effective stress would be a useless concept for non-saturated concrete.

Saturated Concrete.

To decide whether or not the effective stress concept is useful for saturated concrete, it is necessary to answer the question: Is the effective area n' and the strength of interparticle bonds f'_b in cement paste strongly dependent upon pore pressure p ? Lacking direct observations, this question must be answered by deductive reasoning. As long as the deviatoric deformations of concrete remain so small that no appreciable microcracking and volume expansion is produced, the geometry, volume, and surface area of pores filled by water, as well as the microstructure of interparticle bonds and the numbers of water molecules in hindered adsorbed layers, do not change significantly. In such a case, n' and f'_b in Eq. 28 should be approximately constant and the effective stress concept should be applicable, in an approximate sense.

If the overturning failure of a dam is considered, the critical stresses are tensile rather than shearing. When overturning is imminent, concrete is on the verge of tensile failure. This is a type of failure which occurs almost abruptly, with hardly any prior microcracking and volume expansion. Therefore, n' and f'_b should be constant up to the failure

initiation and the effective stress concept should be applicable.

On the other hand, in the case of sliding failure of a dam, formation of a shear band with extensive microcracking causing volume expansion must precede failure (Fig. 2). The increase in pore space alters n' as well as f'_b . At the same time, an immediate drop in pore pressure is produced and possibly even an unsaturated condition (suction) is created. In spite of an increase in n' , the drop in pore pressure would normally reduce the uplift pressure and thus tend to stabilize the material, i.e. stop the shear failure. The saturated condition and the original water pressure is restored only after enough water has been able to seep into the newly created microcracks, which requires considerable time. Therefore, a single short-duration load, such as a single earthquake, is less likely to produce sliding than is the hydrostatic pressure on the upstream face (and this should be reflected in safety factors). After the original pore pressure has been restored, the uplift is larger than before microcracking and the shear failure is likely to continue. Obviously, the concept of effective stress does not suffice to treat the sliding failure, and triaxial stress-strain relations which are valid up to failure and include the pore pressure effect must be developed (see Eqs. 33-38 in the sequel).

Uplift Area.

The question of uplift area n' has been the subject of a long-lasting controversy. Two types of experiments have been conducted to this effect:

1. Fracture produced by pore pressure (e.g. [18]);
2. Deformation produced by pore pressure (e.g. [27]);

Fracture Tests. This method of testing appears natural if one realizes that it is mainly the value of n' at impending tensile failure which is of interest. Perhaps the most careful uplift fracture experiments have been carried out by Leliavski [18]. Their arrangement, shown in Fig. 4, produces a state of stress which closely resembles the conditions existing in concrete of the dam threatened by overturning failure.

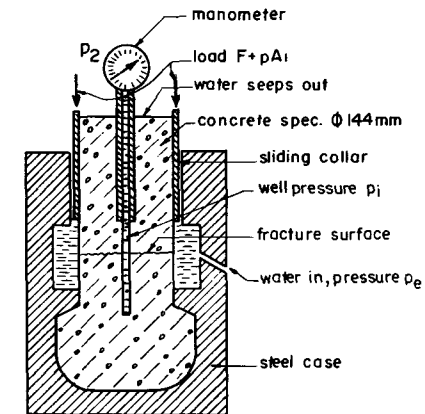


Fig. 4 Simplified Schematic Cross Section of Leliavski's Test Arrangement (1942, 1945) (A_1 = cross section of collar)

The specimens have been subjected to a constant axial load, F_1 , (which is similar to the loading of concrete in dams) and pore water pressure, p , has been slowly induced in the specimen until tensile failure occurred. To eliminate the effect of uncertainty in the strength, f' , of concrete under test conditions, Leliavski calculated n' using two tests with failure pressures p_1 and p_2 under different loads F_1 and F_2 ;

$$n' = \frac{F_2 - F_1}{A(p_2 - p_1)} \quad (29)$$

which ensues by subtracting the equations $n'p_1A = f'A + F_1$ and $n'p_2A = f'A + F_2$ (A = cross section area). The values obtained by testing 95 specimens ranged between 0.85 and 1.00, with the mean value $n' = 0.91$. The upper limit is certainly surprisingly high.

Leliavski reported that equality of the interior well pressure p_i to the external water pressure p_e could never be quite achieved prior to the failure, and he therefore used in Eq. 29 the average value of pore pressure within the cross section, as calculated by formulas for radial seepage flow. However, in the numerous discussions of Leliavski's results it seems to have passed unnoticed that the use of average pore pressure is not the proper assumption. The reason is that tensile fracture always occurs progressively, by propagation of a crack, rather than simultaneously in the whole cross section. Consequently, the fracture must always start at the external surface of the specimen, where the pressure is highest ($p = p_e$, Fig. 4). Once the fracture is initiated, the tensile stress in the remaining cross section is raised (because the total force is constant, assuming the opening of the crack to be negligibly small). Hence, the crack can propagate further, unless the pore pressure ahead of the crack drops too fast, which seems not to have been the case. Apparently, this progressive nature of fracture has been ignored in all the literature on uplift. In the light of the foregoing discussion, Eq. 29 requires the use of the external pressure $p = p_e$ rather than the average pressure in the cross section. If this had been done, Leliavski would have obtained smaller values of n' than he did. Unfortunately, the values of p_e needed to recalculate n' have not been reported in Ref. 18. Part of the scatter of test results may also be due to this fact.

Another difficulty in calculating n' stems from the fact that the pressure difference $p_e - p_i$ must have also some effect on the tensile strength f' . The effect would be vanishing only if p_e equalled p_i (because uniform hydrostatic pressure in the pores is known to have no effect on strength [19, 18]). However, a radial gradient of p produces radial loads (Eq. 26) and so concrete in the core of cross section behaves like concrete under external confining pressure (equal $p_e - p_i$). This must have some, though little known and erratic, effect on tensile fracture.

Leliavski's tests have been criticized for the fact that the n' -value may not indicate the true effective porosity of crack-free concrete, but the effective porosity at the final stage of failure, in which n' is possibly increased by cracking. However, considering the tensile brittleness of concrete (lack of significant microcracking prior to failure), this criticism does not appear to be too serious. To explain it in more detail, consider the increase in pore space (and n') as the tensile crack begins to propagate. At that moment, the pore pressure drops and crack propagation stops. Subsequently, however, it builds up again and as soon as the original value of $n'p$ is attained, which happens at lower p than before, the failure inevitably continues because concrete in tension does not exhibit strain-

hardening, i.e., cracking cannot proceed gradually at increasing strain (in contrast to compression tests). Hence, the original value of $n'p$ at which the cracking started cannot be exceeded at the later stages of failure, which means that the failure test data should lead to the proper value of n' (provided the peak value of pore pressure is used if any drop of p at the end of test is recorded).

Deformation Tests. In view of the possibility that the effective porosity, n' , depends on the tensile stress level, as well as for the purpose of allowable stress design, determination of n' by measuring strain due to pore pressure in the elastic range has been attempted [27, 19, 11, 28, 14]. It will be shown herein, however, that a realistic estimation of n' on the basis of deformation tests is impossible (unless a complete two-phase medium theory were developed). To this end, consider Fig. 5(b). The idea is to calculate from strain ϵ the effective volumetric stress, σ' , in the solid phase of the material, using the known bulk modulus K of the material. Then, knowing σ' and pore pressure p , it is thought that n' could be calculated from the relation $\sigma' = \sigma + n'p$.

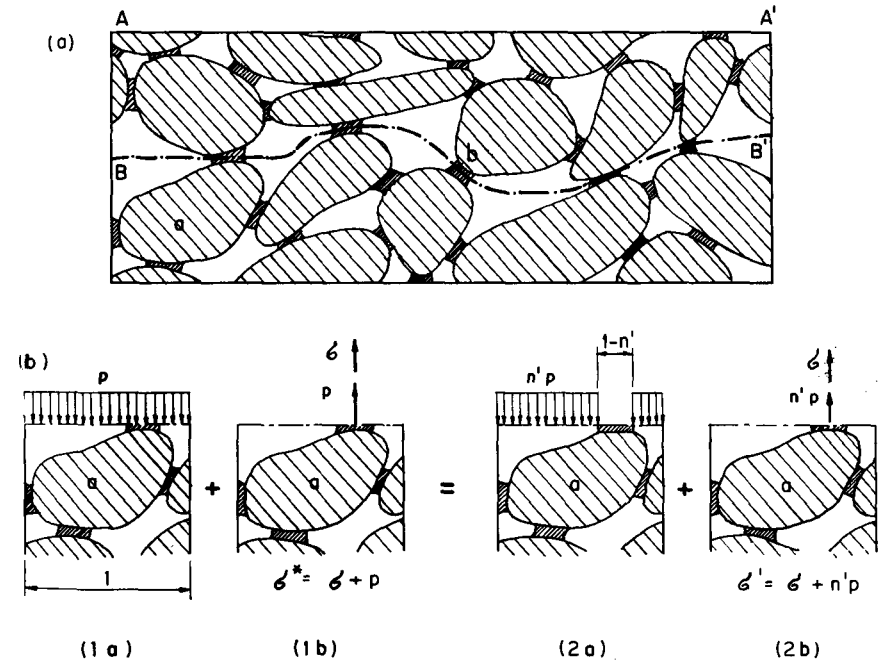


Fig. 5 Idealized Cross Section of a Jointed Granular Material. (a) Cross sections defining $\sigma^s(AA')$ and $\sigma^s(BB')$; (b) Two of the possible decomposition of total stress σ . (This figure does not represent concrete)

This line of thought tacitly implies the assumption that the stress state σ can be decomposed in two stress states, exemplified by states 2a and 2b in Fig. 5, of which only one state, 2b, contributes appreciably to the overall deformation, ϵ , of the porous solid, while the other state, 2a, contributes negligibly to the deformation. However, the stress

state σ can be also decomposed in other ways, and one alternative decomposition is shown by states 1a and 1b. In the case 1a, grain a is subjected to pressure p on all of its boundary, and thus the material of the grain must be in a purely volumetric state of stress, i.e. free of shear stresses. In the case 2b, grain a is not loaded by p over all its surface and is not in a purely volumetric state of stress, so that shear stresses must also exist within the grain. These tend to be concentrated near interparticle joints, which should lead to a considerably larger overall strain of the porous solid than does the purely volumetric stress state in the grains. It is generally true of most porous materials that their overall volumetric deformation is mostly due to localized microscopic shear stresses within the microstructure and the volume compressibility of the solid matter forming the porous material is usually much less than the volume compressibility of the porous material on the whole. It is hard to check this condition for concrete because the volume compressibility of cement gel particles is not known. However, concrete is probably an extreme case for which the difference between the two compressibilities is small, due to the fact that cement gel particles are bonded across hindered adsorbed water layers. Nevertheless, among cases 1a and 2a, it should be case 1a which leads to smaller overall deformation of the porous solid. In any event, case 2b (with $\sigma' = \sigma + n'p$), implied in the analyses thus far, is not closer to reality than case 1b. The reality should be between cases 1b and 2b, probably closer to case 1b. In consequences of these facts, the volumetric strain ϵ due to pore pressure p and applied total stress σ may be best approximated as

$$\epsilon \approx \sigma^*/3K \quad \text{with } \sigma^* \approx \sigma + p \quad (30)$$

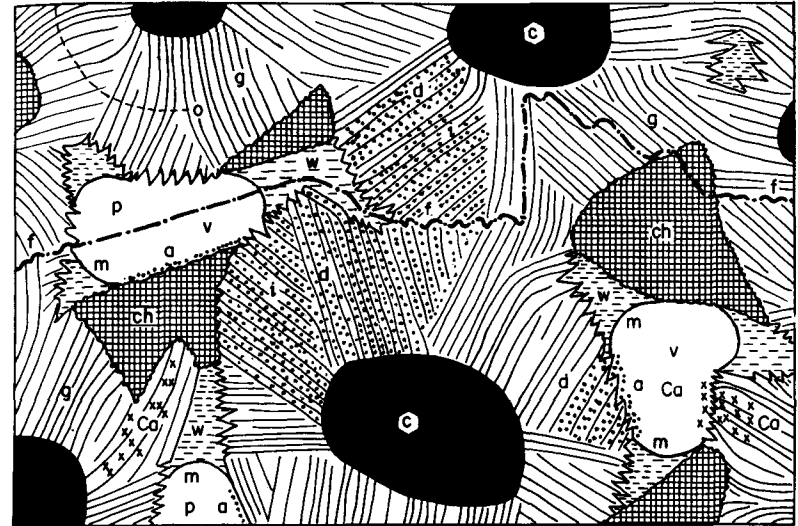
where K = bulk modulus of concrete at constant p .

Eq. 30 does not contain n' , and so n' cannot be evaluated from test data on deformation ϵ produced by pore pressure, unless a more accurate equation is deduced. Nevertheless, the deformation tests are useful for determining the value of $\partial\epsilon/\partial p$ which is requisite for calculating the strains and stresses in the dam due to pore pressures. In Ref. 8 (Eq. 55), it has been demonstrated that for sand ($n' \approx 1$) the coefficient $\partial\epsilon/\partial p$ at constant total stress σ very nearly equals $1/K$, the bulk compressibility of the saturated sand. Based on the preceding consideration relative to Fig. 5(b), $\partial\epsilon/\partial p$ should not be much different when $n' < 1$. Thus, it is the fact that $\partial\epsilon/\partial p$ is nearly independent of n' which makes it impossible to reliably determine n' from deformation tests.

In the light of the foregoing discussion, it is not surprising that the scatter of the n' -values obtained from deformation tests has been large, despite greatest care. Some of the calculated values [27, 19, 11, 28, 14] have even exceeded 1.0, some have been much less than 1.0, and frequently they were close to 1.0 [28].

The stress state decomposition in Fig. 5 may also be considered in failure analysis. It is well known [18] that concrete (as well as rocks) has the same strength when the specimen is submerged under water of pressure p , provided pore pressure also reaches p . Here, case 1a (Fig. 5) is that which indicates the stress state prior to applying axial load under water, and indeed, this stress state can have no effect on failure because the grains are in a volumetric state of stress and the joints are stress-free.

Conclusions from Cement Paste Microstructure. The fracture surfaces in dam concretes are known to hardly ever pass through the aggregate. Therefore, the effective stress and uplift in concrete is the same as in cement paste. Powers [25] analyzed the chemical bond-



Idealized Schematic Microstructure of Hardened Portland Cement Paste; a = free adsorbed water molecules, Ca = calcium ions (crosses), c = remaining anhydrous cement, ch = calcium hydroxide, d = hindered adsorbed water molecules, f = fracture surface, g = cement gel (lines represent sheets of calcium silicate hydrates), i = interlayer water, m = capillary meniscus, o = original surface of unhydrated cement grains, p = capillary pore, v = water vapor and air, w = capillary (liquid) water. Water molecules and calcium ions are not shown everywhere they exist. Width of picture $\approx 30 \mu\text{m}$. Spacing of sheets ($\sim 30 \text{ \AA}$) relative to length of sheets is about 100-times exaggerated.

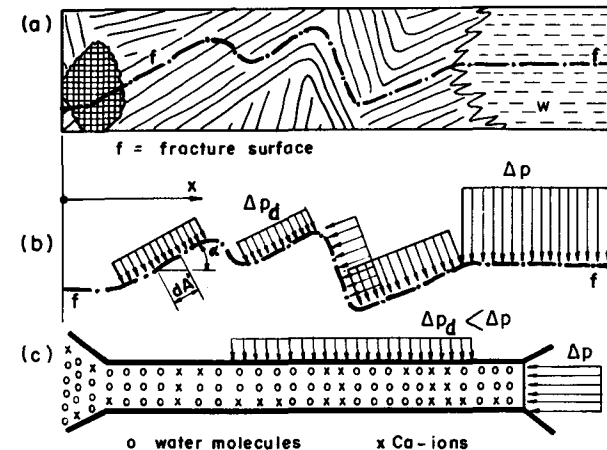


Fig. 7 (a)-(b) Example of the Fracture Surface in Hardened Cement Paste (cf. Fig. 6), (c) Hindered Adsorbed Water Layer

ing of gel particles in cement paste. Considering the particles to be spheroidal with about 12 monoatomic chemical bonds, and taking into account the average size of gel particles, he concluded that the bonded surface area of each particle is only about 0.2 percent of the total surface area, leaving thus 0.998 of the surface area accessible to water. However, it seems to have been overlooked thus far that this result does not imply that $n' = 0.998$. This is due to the fact that anisotropic, rather than isotropic (hydrostatic), states of stress must exist in all pores whose thickness l is less than ten molecular diameters (26.3×10^{-10} m). These pores represent what is known as hindered adsorbed water layers [5] and include both the physically adsorbed water and the interlayer water (d and i in Fig. 6). Consider the hindered adsorbed layer in Fig. 7(c). As soon as the pressure p of water in an adjacent macropore (capillary pore) is raised, water molecules begin migrating along the solid surface into the adsorbed layer until a constant value of Gibb's free energy μ throughout the layer is reached. At constant temperature, the attainment of constant μ means that the spreading pressure, π_d , of water molecules is such that the average longitudinal pressure p in the layer ($p = \pi_d/l$) is constant (see Eqs. 18, 22 and 29 or Ref. 4). Adsorbed water molecules are not freely mobile in all directions, unlike those in liquid (capillary) water. Their movement is completely restricted in the direction normal to the layer and is also largely restricted within the plane of the layer (especially in the first molecular layer), due to the periodicity of the potential of adsorption forces at the solid surface. By virtue of this fact, water in the hindered adsorbed water layer resembles more a solid than a liquid, especially in the transverse direction. Hence, the state of (average) stress in the layer need not be hydrostatic. In particular, if pressure increment Δp is applied in the directions of the surface (Fig. 7(c)), the increment Δp_d of p_d (called disjoining pressure) must be less than Δp , as it would be in a solid; hence $\Delta p_d = \nu' \Delta p$ where $\nu' < 1$ is a parameter analogous to Poisson's ratio of solids and depending on the thickness l of the layer.

A significant portion of the fracture surface through cement gel is likely to pass along hindered adsorbed water layers; see Fig. 7(a). On this portion, the pressures acting on the surface just prior to fracture are $\Delta p_d = \nu' \Delta p$. The condition of static equivalence of macroscopic and microscopic stresses acting on the failure surface yields $\Delta \sigma = \Delta \sigma' - n_c p - \int_{n_d} \nu' p_d \cos \alpha \, dA'$ (Fig. 7(b)) where n_c = portion of the sinuous fracture surface (f - f in Fig. 6) passing through capillary water and n_d = portion passing along hindered adsorbed layer; dA' = microscopic area element of the sinuous fracture surface and α = its angle with the macroscopic fracture plane. Obviously $n_c + n_d < 1$; probably $n_c + n_d$ is quite close to unity. Substituting $\Delta \sigma = \Delta \sigma' - n' \Delta p$ (Eq. 24), it follows

$$n' = n_c + \nu'_{av} n_d, \quad \text{with } \nu'_{av} n_d = \int_{n_d} \nu'(l) \, dA \quad (31)$$

in which $dA = dA' \cos \alpha$ = area element of macroscopic fracture plane; l = function of coordinates x and y on this plane; and ν'_{av} = average value of ν' for the hindered adsorbed layers. Because $\nu'_{av} < 1$, a typical value being perhaps 0.6, it becomes clear that the uplift area n' must be substantially smaller than one, even if most of the fracture surface passes through water (as Powers assumed). This is, of course, true only for uninjured cement paste and concrete. Eq. (31) may allow a quantitative estimate of n' if a sufficient quantitative know-

ledge of the microstructure of cement paste is attained.

The migration of water molecules into the hindered adsorbed water layers is a slow process. The changes Δp_d in disjoining pressure p_d occur with a substantial delay after the change Δp of pressure p in the capillary pores. Thus, at the instant the change Δp occurs, the uplift area n' for that change is only n_c , and the value of n' indicated by Eq. 31 is approached only after a certain time. This time should be about the same as the lag of the delayed component of shrinkage behind the change in pore humidity, and this suggests a delay of a few months. This delay is not large as compared with the time needed for the pressure to penetrate the concrete of the dam, but may be large in case of laboratory tests.

TRIAXIAL STRESS-STRAIN RELATIONS AND FAILURE ANALYSIS

The failure analysis of a dam, especially analysis of the sliding failure, requires the knowledge of realistic non-linear triaxial stress-strain relations of the material. When the effect of pore pressure is negligible, these relations may be in general written in the form

$$de_{ij} = \frac{ds_{ij}}{2G} + de''_{ij}, \quad d\epsilon = \frac{d\sigma}{3K} + d\lambda \quad (32)$$

in which $s_{ij} = \sigma_{ij} - \delta_{ij}\sigma$ = deviator of stress tensor σ_{ij} ; $de_{ij} = \epsilon_{ij} - \delta_{ij}\epsilon$ = deviator of strain tensor ϵ_{ij} ; de''_{ij} = deviatoric inelastic strain increments, $d\lambda$ = inelastic dilatancy [6, 7] (resulting from deviatoric strains). The time-dependent strains (creep and shrinkage) as well as thermal strains, are not considered herein.

When pore pressure changes are important, a rigorous approach requires a two-phase medium model (Eq. 39 in the sequel). However, the one-phase medium model (Eq. 32) may still be used as a simple approximation. For this purpose, it is necessary to decide whether σ should remain in Eq. 32 or be replaced by $\sigma + p$ or $\sigma + n'p$, and also which type of stress should be used in calculating $d\lambda$. Recalling the discussion that has led to Eq. 30, the most appropriate formulation appears to be as follows:

$$de_{ij} = \frac{d\sigma^*_{ij}}{2G} + de''_{ij}, \quad d\epsilon = \frac{d\sigma^*}{3K} + d\lambda + C dp, \quad \text{with } \sigma^* = \sigma + p \quad (33)$$

in which σ^* , the effective stress for $n' = 1$, is used to determine the elastic strains (same as for sands; see Eq. 19 of Ref. 14); and $C = \partial\epsilon/\partial p$ at constant σ^* , as determined by tests of deformation due to pore pressure. The inelastic strains also depend on volumetric stress. However, inasmuch as the inelastic strains are due to microcracking, de''_{ij} and $d\lambda$ ought to be determined with the help of the effective stress $\sigma' = \sigma + n'p$ (rather than σ^*) because this stress governs fracture. A specific formulation will be given in the sequel.

Formulation of the stress-strain relations for concrete (with negligible pore pressures) has recently been intensely studied. Applications of the theories of plasticity and hypoelasticity have met with a limited success. However, an entirely new formulation, called endochronic theory, was proposed in 1974 for concrete [6, 7]. In this formulation, the accumulation of damage due to microcracking is described by means of the variable, ξ , defined as

$$d\xi = \sqrt{\frac{1}{2} de_{ij} de_{ij}} \quad (34)$$

and the inelastic strain increments, in the special case of time-independent formulation, are expressed as

$$de''_{ij} = \frac{s_{ij}}{2G} dz, \quad dz = \frac{d\eta}{f(\eta)}, \quad (35)$$

$$d\eta = F(\epsilon_{ij}, \sigma) d\xi, \quad d\lambda = F_1(\lambda, \epsilon_{ij}, \sigma) d\xi \quad (36)$$

$$G = G(\lambda), \quad K = K(\lambda) \quad (37)$$

Here z = intrinsic time; f , F , F_1 = isotropic functions which must be determined experimentally; and G , K = incremental shear modulus and bulk modulus, which both depend on dilatancy λ (due to microcracking). It has been demonstrated [7] that virtually all known basic behavior of concrete (stress-strain curves and failure data for compression, tension, biaxial and triaxial tests, lateral strains, volume change, torsion with compression, unloading, cyclic loading, spirally reinforced and spirally prestressed concrete) can be adequately modeled by Eqs. 32 and 34-37.

For an approximate extension of the endochronic stress-strain law to the case of large pore pressures, Eq. 32 is replaced by Eq. 33, as has already been mentioned. Furthermore, stress σ appearing in the argument of functions F and F_1 should be replaced not by σ^* but by $\sigma' = \sigma + n'p$ because σ in these two functions describes the effect of confining pressure on microcracking, which is a fracture-type phenomenon and thus depends mainly on σ' , according to Eq. 27. Hence, an approximate extension of the endochronic law to large pore pressures also requires that Eq. 36 be replaced by

$$d\eta = F(\epsilon_{ij}, \sigma') d\xi, \quad d\lambda = F_1(\lambda, \epsilon_{ij}, \sigma') d\xi, \quad \text{with } \sigma' = \sigma + n'p \quad (38)$$

In a rigorous formulation, the concept of an inelastic two-phase medium must be used. In this concept, which has already been developed for saturated sands [8], the volumetric stress-strain relation from Eq. 33 must be replaced by the relations

$$d\epsilon^S = C_{11} d\sigma^S + C_{12} d\sigma^F + d\lambda \quad (39)$$

$$d\epsilon^F = C_{21} d\sigma^S + C_{22} d\sigma^F - kd\lambda$$

in which ϵ^S , ϵ^F = strains in solid and fluid; σ^S , σ^F = the associated stresses in solid and fluid (Eq. 20); C_{11} , C_{12} , C_{21} , C_{22} = elastic compressibilities ($C_{12} = C_{21}$); k = experimental coefficient characterizing the strain of fluid which is necessary to allow the inelastic strain of solid, $d\lambda$, to occur at constant σ^S and σ^F . Eq. 39 cannot be practically used as yet, because the values of C_{11} , C_{12} , C_{21} , C_{22} and k are not known.

There are several other material properties that are of interest for the analysis of gravity dams, but are beyond the scope of this paper. These include: effects of creep, shrinkage, and hydration heat on the stresses and cracking; and propagation of cracks across the dam, with the influence of temporary pore suction caused by volume increase near the tip of crack. One particularly noteworthy difficulty in analyzing the crack propagation is the fact that, owing to the very large size of dams relative to the size of aggregate, a singular stress field can develop near the crack tip (around a small zone of microcracking). Another facet of this phenomenon is the unstable strain localization (material instability) when tangent moduli become very small (as it happens on approach to failure). This phenomenon cannot occur on a scale that is not sufficiently large as com-

pared with the size of aggregate, and is insignificant in ordinary-size reinforced concrete structures, whereas in structures as large as dams this phenomenon should be of importance. The usual finite element method cannot account for this effect, unless the size of finite elements does not exceed about 20-times the size of aggregate, which is an impossibly small limit for the analysis of a dam. Special methods will have to be developed for this purpose if the analysis up to failure (e.g., sliding failure) should yield realistic results.

CONCLUSIONS

1. In an ideal dam, which is free of cracks, the rate of penetration of hydraulic overpressure p into concrete is extremely slow. This is due to the water deficiency of concrete which is caused by hydration (self-desiccation), and even more, by air-entrainment. Only about $\frac{1}{2}$ thickness of a large ideal dam can be penetrated within 100 years, the rest remaining unsaturated. (In a real dam, the spacing and width of continuous cracks through the dam, whether in concrete or in construction joints, and the type of drainage normally dominate the rate of saturation of concrete within the dam.)
2. Drying from the downstream face is even slower and normally cannot penetrate deeper than a few meters into an ideal dam within a 100-year time span. When saturated cracks extend to the downstream face, the penetration of drying is still much smaller. Therefore, drying has a relatively small effect on uplift distribution and shrinkage stresses in the dam are small, except near the face (and near construction joints, due to drying during construction).
3. It is shown that the water deficiency, which is continuously being created by hydration, must be included in the linear diffusion equation governing pore pressures in saturated concrete. This effect substantially reduces pore pressures and may often cause unsaturated condition. The movement of saturation boundary complicates solution, but approximately a water sink equivalent to terminal water deficiency of concrete may be assumed to exist at the moving saturation boundary. More accurately, water diffusion in non-saturated concrete ahead of the saturation boundary is to be considered, with a proper interface condition (Eq. 18).
4. When diffusivity C of saturated concrete is calculated from its permeability c , the value of compressibility β which relates C to c (Eq. 4) must take into account: (1) the fact that only the volume change of capillary water should be included in β , while the hindered adsorbed water forms essentially part of the solid structure and should not be included; (2) the dilation of pore space due to deformation of solid under pore pressure.
5. Although the diffusivity C' in non-saturated concrete is strongly dependent on pore humidity (Eq. 13), most of the mass of the dam (downstream surface layer excepted) falls into the region of constant C' , in view of the high pore humidities after self-desiccation.
6. Despite the fact that over 99% of the weakest microscopically sinuous cross section of concrete passes through water, the effective uplift area n' must be distinctly less than 1.0. This ensues from the fact that the transverse pressure which is induced in hindered adsorbed water layers by the pressure Δp in capillary pores must be substantially less than Δp , due to the non-liquid nature of adsorbed water layers. A reasonable estimate seems to be $n' = 0.9$ when safety against tensile fracture is analyzed.

7. Tests of deformation due to pore pressure cannot yield the value of effective uplift area n' , unless a two-phase medium model is developed for concrete. Among the simplified assessments of the effective uplift area for deformation analysis (Fig. 5), 1.0 is the most reasonable value.

8. At the present level of knowledge, only failure tests are useful for determining the uplift area. In their evaluation, it is necessary to take into account the progressive nature of fracture when there is pressure gradient along the fracture surface.

9. No "negative" uplift should be introduced due to gradients of pore tensions in drying concrete. This effect is accounted for by including shrinkage strains in the analysis.

10. In the range of confining pressures within dams, concrete cannot fail by shear (sliding) without prior volume expansion due to microcracking. For this reason, the uplift area determined from tests of failure due to pore pressure is of no relevance for shear failures, in contrast to overturning failure. When the safety against shear (sliding) failure is analyzed, the gradual development of microcracks prior to failure must be taken into account. This means that the effective porosity n' approaches 1.0. However, the temporary pore suction produced by volume expansion (dilatancy) due to shear (microcracking), which temporarily reduces the uplift pressure, should also be considered.

11. The progressive nature (propagation) of the tensile fracture (overturning failure), as well as the shear fracture (sliding failure), should be considered in an accurate analysis.

12. To extend the nonlinear incremental triaxial stress-strain relations for concrete to the case of large pore pressures, one may, as an approximation, replace the volumetric stress increments in concrete by the effective stress for the effective porosity 1.0. However, the total (non-incremental) volumetric stress appearing in the expressions for inelastic deviator strains and dilatancy should be replaced by the effective stress for the actual effective porosity n' ($n' \approx 0.9$). The deformations due to pore pressure changes represent an additional term in the stress-strain relation. For a rigorous formulation, a two-phase medium formulation would have to be verified experimentally.

Conclusions 1, 2, 5, and 9-11 summarize the facts already in essence known. Conclusions 3, 4, 6-8, and 12 are based on the present analysis.

Acknowledgement.

The support of the U.S. National Science Foundation under Grant GK-26030 is gratefully appreciated.

REFERENCES

1. Aleksandrovskii, S.V., "Analysis of Plain and Reinforced Concrete Structures for Temperature and Moisture Changes with Account of Creep" (in Russian), 2nd Ed., Stroyizdat, Moscow, 1973 (Chpt. II).
2. Bažant, Z.P., Najjar, L.J., "Drying of Concrete as a Nonlinear Diffusion Problem," Cement & Concrete Research, Vol. 1, 1971, pp. 461-473.
3. Bažant, Z.P., Najjar, L.J., "Nonlinear Water Diffusion in Nonsaturated Concrete," Materials and Structures (RILEM, Paris), Vol. 5, 1972, pp. 3-20.
4. Bažant, Z.P., "Thermodynamics of Interacting Continua with Surfaces," Nuclear Engineering and Design, Vol. 20, 1972, pp. 477-505.

5. Bažant, Z.P., "Theory of Creep and Shrinkage in Concrete Structures: A Précis of Recent Developments," Mechanics Today, Vol. 2, pp. 1-93, Pergamon Press, 1975.
6. Bažant, Z.P., "A New Approach to Inelasticity and Failure of Concrete, Sand and Rock: Endochronic Theory," Proc. Soc. of Engng. Science 11th Annual Meeting, G.J. Dvorak, Ed., Duke University, Durham, N.C., Nov. 1974, pp. 158-159.
7. Bažant, Z.P., "Endochronic Theory for Inelasticity and Failure of Concrete," submitted to Proc. ASCE, J. Eng. Mech. Div.
8. Bažant, Z.P., Krizek, R.J., "Saturated Sand as an Inelastic Two-Phase Medium," J. Eng. Mech. Div., Proc. ASCE, Vol. 101, 1975 (in press).
9. Biot, M.A., "Theory of Propagation of Elastic Waves in a Fluid-Saturated Porous Solid," J. of the Acoustical Soc. of Am., Vol. 28, 1956, pp. 168-191.
10. Bhatnagar, P.S., Kapla, I.P., Sharma, R.P., "Structural Behavior of Bhakra Dam," Int. Comm. on Large Dams, 9th Congress, Istanbul, 1967, Vol. III, pp. 245-274.
11. Carlson, W., Davis, R.E., Discussion, Proc. ASCE, Vol. 74, 1948, p. 1532.
12. Carlson, R.W., "Permeability, Pore Pressure, and Uplift in Gravity Dams," Trans. ASME, Vol. 122, 1957, pp. 587-613.
13. Crank, J., Mathematics of Diffusion, Oxford University Press, London 1957.
14. Fillunger, P., "Versuche über die Zugfestigkeit bei allseitigen Wasserdruck," Oester. Wochenschrift für den Öffentl. Baudienst, Vol. 29, 1915, p. 443.
15. Italian Subcommittee for Observations of Dams, "Dam Measurements in Italy," Int. Comm. on Large Dams, 8th Congress, Edinburgh, 1964, Vol. 2, pp. 684-686.
16. Joint ASCE-USCOLD Committee on Design, "Design Criteria for Large Dams," ASCE, New York, 1967, p. 92 and p. 97 (see also "Final Report of the Subcommittee on Uplift in Masonry Dams," ASCE Separate No. 133, and Trans. ASCE, Vol. 117, 1952, p. 1218).
17. Lacy, F.P., Schoick, G.L.V., "T.V.A. Concrete Gravity Dams Uplift Observations and Remedial Measures," Int. Comm. on Large Dams, 9th Congress, Istanbul, 1967, Vol. 1, 487-507.
18. Leliavski, S., Uplift in Gravity Dams, Constable & Co. Ltd., London 1958; see also Trans. ASCE, Vol. 112, 1947, pp. 444-487; and a summary in: N.S. Attri, "Uplift in Gravity Dams," J. Struct. Div., Proc. ASCE, Vol. 93, 1967, pp. 61-68.
19. McHenry, D., "The Effect of Uplift Pressure on the Shearing Strength of Concrete," 3rd Congress, Int. Comm. on Large Dams, Stockholm, 1948, Vol. I, R. 48.
20. Mather, B., "Use of Low Portland Cement Content in Construction of Dams," J. Am. Concrete Institute, Vol. 71, 1974, pp. 589-599.
21. Murata, J., "Studies of the Permeability of Concrete," Bulletin RILEM (Paris) No. 29, Dec. 1965, pp. 47-54.
22. Nicol, T.B., et al., "Deterioration Problems at Avon Dam," Int. Comm. on Large Dams, 9th Congress, Istanbul, 1967, Vol. III, p. 716.
23. Powers, T.C., "A Discussion of Cement Hydration in Relation to the Curing of Concrete," Proc. of the Highway Research Board, Vol. 27, 1947, pp. 178-188 (also PCA Bull. 25).
24. Powers, T.C., Copeland, L.E., Hayes, J.C., Mann, H.M., "Permeability of Portland Cement Paste," J. Am. Concrete Inst., Vol. 51, 1954, pp. 285-298 (also PCA Bull. 53).
25. Powers, T.C., "Hydraulic Pressure in Concrete," Proc. Am. Soc. of Civil Engrs., Vol. 81, July 1955, Paper 742 (also PCA Bull. 63).
26. Rhodes, J.A., "Structural Behavior Measurements on Concrete Gravity Dams," Int. Comm. on Large Dams, 8th Congress, held in Edinburgh, 1964, Vol. II, pp. 125-142.

27. Serafim, J.L., "The 'Uplift Area' in Plain Concrete in the Elastic Range," Int. Comm. on Large Dams, 8th Congress, held in Edinburgh, 1964, Vol. 5, Comm. 17, pp. 599-622; also: "Déformations du béton dues aux pressions dans les pores," Bull. RILEM, No. 27, 1965, pp. 73-76.
28. Terzaghi, K., "Simple Tests to Determine Hydrostatic Uplift," Engng. News Record, June 18, 1936, p. 872.
29. Terzaghi, K., "Stress Conditions for the Failure of Concrete and Rock," Proc. ASTM, Vol. 45, 1945, p. 777.
30. Wierig, H.J., "Die Wasserdampfdurchlässigkeit von Zementmörtel und Beton," Zement-Kalk-Gips, 1965, No. 9, pp. 471-482.
31. Zienkiewicz, "Stress Analysis of Hydraulic Structures Including Pore Pressure Effects," Water Power (London), Vol. 15, No. 3, March 1963.

APPENDIX I - NUMERICAL ANALYSIS OF WATER DIFFUSION IN DAMS

To develop a finite element program covering water diffusion in both saturated and non-saturated concrete, it is advantageous to put the governing differential equations for each of these two cases into a common form. This form reads

$$J = -A \text{ grad } X, \quad B \frac{\partial X}{\partial t} - H' = -\text{div } J \quad (40)$$

in which X is the unknown field variable; A and B = given coefficients, and $H' = H'(t)$ = given function of time. As can be easily verified, Eqs. 40 reduce to Eqs. 11 and 12 for $X < 0$ and to Eqs. 2 and 3b for $X \geq 0$, if the following definitions are introduced:

$$\text{for } X < 0: X = h-1, \quad A=c', \quad B = \frac{1}{k} = \frac{c'}{C'}, \quad H' = \frac{1}{k} \frac{\partial h_s}{\partial t} \quad (41)$$

$$\text{for } X \geq 0: X = p, \quad A = \frac{\rho_w}{g_w} c, \quad B = \frac{\rho_w c}{g_w C}, \quad H' = \frac{\partial w}{\partial t} \quad (42)$$

The interface condition for the saturation boundary (Eq. 18) is automatically satisfied. The boundary conditions at the upstream and downstream faces of the dam consist in a prescribed value of X , while on the foundation surface the normal component of $\text{grad } J$ either is zero or is continuous across the surface.

The finite element formulation for equations of the type 40 is well known. Eq. 40 has the advantage that a single type of finite element covers both saturated and unsaturated condition. Also, restricting the saturation boundary to lie on the element boundary, the interface condition (Eq. 18) is automatically satisfied by the finite element formulation. Time integration is carried out in steps and several iterations are necessary at each step to determine whether A , B , and F' should be computed from Eq. 42 or Eq. 43.

The effect of temperature gradients (due to hydration heat) upon moisture diffusion ought to be also considered if an accurate prediction of early pore pressure development is desired. This problem is beyond the scope of this study.

APPENDIX II - BASIC NOTATIONS

- c, c', c^* = permeability coefficients in Eqs. 2, 11, and 1;
- C, C' = diffusivity of saturated and non-saturated concrete (Eqs. 4, 12, 13);
- C'_1 = value of C' at saturation;
- g_w = specific weight of liquid water;
- h = relative humidity in the pores;
- h_s = h produced by self-desiccation at constant \bar{w} (Eq. 12)
- \vec{J} = vector of the mass flux of water in concrete;
- k = inverse slope of desorption or adsorption isotherm (Eq. 16)
- K = bulk modulus of concrete (Eq. 30);
- n, n' = volumetric porosity and effective porosity (Eqs. 20, 24);
- p = pressure in capillary pores (in excess of one atmosphere);
- p_0 = value of p at the boundary;
- t = time;
- U_i, U'_i = uplift body forces (Eqs. 23, 26);
- w, \bar{w} = masses of capillary water and of all water per m^3 of concrete;
- w_h = water deficiency produced by hydration (Eq. 3b);
- x, y or x_i = cartesian spatial coordinates ($i = 1, 2, 3$);
- β, β_w = compressibilities of pore water phase and of liquid water as such;
- ϵ_{ij}, ϵ = strain tensor and volumetric strain;
- μ = Gibbs' free energy per unit mass of pore water;
- ρ_w = mass density of liquid water; ρ^F, ρ^S, ρ = bulk mass densities of the fluid phase, solid phase; and concrete as a whole;
- Superscripts $(..)^F, (..)^S$ refer to fluid phase and solid phase.

APPENDIX III - NOTE AFTER SUBMISSION OF MANUSCRIPT

As a reaction to several valuable comments which the writer had the privilege receive from Messrs. Bryant Mather and Roy W. Carlson after their glancing over the manuscript, the writer wishes to correct one statement and expand others.

The value of 6% as the typical air-entrainment of concrete is unrealistic. Actually, this value is typical of the fraction of the fresh mixture which passes the 1.5-inch sieve. In the full mixture with 6-inch aggregate, this corresponds to roughly 3 to 3.5% air-entrainment and thus all numerical values given before relative to air-entrainment should be corrected accordingly. However, the corrections are not significant and do not change any of the conclusions.

It must be emphasized that there is no direct experimental support for the 600 fold increase in permeability on saturation, as mentioned below Eq. 19. This is merely an indirect logical inference from certain isolated test data for different concretes and the explanation in terms of microstructure below Eq. 19 is merely tentative. However, no data contradicting this inference are known either.

It should be also noted that self-desiccation slows down hydration, which in turn slows down self-desiccation and development of water deficiency. Thus, function $f(t)$ mentioned before Eq. 4 should depend not only on temperature but also on h , which may be done by replacing $f(t)$ by $f(t, h)$, t being the equivalent hydration period [5]. Nevertheless, except for extremely low water-cement ratios, the drop of pore humidity due to self-desiccation is only a few percent, which would not have much effect on $f(t)$.

The water deficiency need not be strictly proportional to the cement content when pozzolans are present because the pozzolans might not be inert in the hydration process. The estimate of 3 kg/m^3 water deficiency before Eq. 4 may be too low, although it should be good enough for the purpose of the present analysis.

Perhaps it should be also emphasized that the overturning failure is considered only for the purpose of determining the safety against this failure to occur because even 100% uplift over the entire base cannot overturn the dam. Also, the safety against sliding failure is normally more critical.

The statement (below Eq. 30) that fracture hardly ever passes through the aggregate is based on the experimental data (of S. Shah, G. Winter, and others) which indicate that in low strength concretes, by contrast to high stress concretes, microcracking begins at the aggregate-mortar interface and then spreads into the mortar.

Errata. - In Fig. 1, change "unhydrous" to "anhydrous" and "cement gel" to "cement gel with other hydration products", more accurately. In the 2nd line below Eq. 16, insert comma before w_{ev} . In Ref. 31 - insert author's initials O.C.